0090-9556/10/3806-963–972$20.00
DRUG METABOLISM AND DISPOSITION
Vol. 38, No. 6
32391/3586530
DMD 38:963–972, 2010
Printed in U.S.A.

Sequential Metabolism of Secondary Alkyl Amines to Metabolic-Intermediate Complexes: Opposing Roles for the Secondary Hydroxylamine and Primary Amine Metabolites of Desipramine, (*S*)-Fluoxetine, and *N*-Desmethyldiltiazem

Kelsey L. Hanson, Brooke M. VandenBrink, Kantipudi N. Babu, Kyle E. Allen, Wendel L. Nelson, and Kent L. Kunze

Department of Medicinal Chemistry, School of Pharmacy, University of Washington, Seattle, Washington

Received January 22, 2010; accepted March 3, 2010

ABSTRACT:

Three secondary amines desipramine (DES), (*S*)-fluoxetine [(*S*)-FLX], and *N*-desmethyldiltiazem (MA) undergo *N*-hydroxylation to the corresponding secondary hydroxylamines [*N*-hydroxydesipramine, (*S*)-*N*-hydroxyfluoxetine, and *N*-hydroxy-*N*-desmethyldiltiazem] by cytochromes P450 2C11, 2C19, and 3A4, respectively. The expected primary amine products, *N*-desmethyldesipramine, (*S*)-norfluoxetine, and *N,N*-didesmethyldiltiazem, are also observed. The formation of metabolic-intermediate (MI) complexes from these substrates and metabolites was examined. In each example, the initial rates of MI complex accumulation followed the order secondary hydroxylamine > secondary amine ≫ primary amine, suggesting that the primary amine metabolites do not contribute to formation of MI complexes from these secondary amines. Furthermore, the primary amine metabolites, which accumulate in incubations of the secondary amines, inhibit MI complex formation. Mass balance studies provided estimates of the product ratios of *N*-dealkylation to *N*-hydroxylation. The ratios were 2.9 (DES-CYP2C11), 3.6 [(*S*)-FLX-CYP2C19], and 0.8 (MA-CYP3A4), indicating that secondary hydroxylamines are significant metabolites of the P450-mediated metabolism of secondary alkyl amines. Parallel studies with *N*-methyl-d_3-desipramine and CYP2C11 demonstrated significant isotopically sensitive switching from *N*-demethylation to *N*-hydroxylation. These findings demonstrate that the major pathway to MI complex formation from these secondary amines arises from *N*-hydroxylation rather than *N*-dealkylation and that the primary amines are significant competitive inhibitors of MI complex formation.

The metabolism of alkyl amine-containing drugs leads to the formation of primary and secondary metabolites, which include *N*-dealkylated, *N*-hydroxylated, and *N*-oxygenated species (Lindeke et al., 1979; Franklin, 1995). Further oxidation of these metabolites leads to time-dependent inhibition (TDI) of cytochrome P450 (P450) enzymes because of the formation of metabolic-intermediate (MI) complexes (Fig. 1). MI complexes exhibit a signature Soret absorbance at approximately 455 nm (Franklin, 1974). Predictions of the magnitude of drug-drug interactions (DDIs) for diltiazem, fluoxetine, and clarithromycin have been reported using results from in vitro kinetic studies and from measured alkyl amine concentrations in vivo (Mayhew et al., 2000; Galetin et al., 2006; Zhang et al., 2009b).

Mapping the oxidative pathways that drive MI complex formation and defining the roles of the metabolites will be beneficial in devising better methods for the prediction of DDIs. The complexity of the alkyl amine metabolic pathways is a barrier to the rational prediction of DDIs (Fig. 1). The study of the pathways of metabolism in single enzyme systems is a logical first step to improve current predictive efforts. Proof that a single P450 catalyzes all of the steps required for MI complex formation from a tertiary amine was obtained more than three decades ago (Kawalek et al., 1976). More recent results from several laboratories show that a number of alkyl amine metabolites

This work was supported by the National Institutes of Health National Institute of General Medical Sciences [Project Program Grant P01-GM32165, Pharmacological Sciences Training Grant T32-GM007750] (to B.M.V. and K.E.A.).

K.L.H. and B.M.V. contributed equally to this work.

Parts of this work were previously presented at the following conference: Hanson KL, Zhao P, Babu KN, Nelson WL, Kalhorn TF, and Kunze KL (2008) Time-dependent inhibition of CYP3A by diltiazem: the role of the sequentially-formed metabolite, *N*-hydroxydesmethyl diltiazem, in MI complex formation and VandenBrink BM, Babu KN, Isoherranen N, Nelson WL, Kalhorn TF, and Kunze KL (2008) Stereoselective metabolism of fluoxetine results in irreversible inhibition of CYP2C19 through the formation of an MI complex. *15th Annual International Society for the Study of Xenobiotics Meeting*; 2008 Oct 12–16; San Diego, CA. International Society for the Study of Xenobiotics, Washington, DC.

Article, publication date, and citation information can be found at http://dmd.aspetjournals.org.

doi:10.1124/dmd.110.032391.

ABBREVIATIONS: TDI, time-dependent inhibition; P450, cytochrome P450; MI complex, metabolic-intermediate complex; DDI, drug-drug interaction; DES, desipramine; (*S*)-FLX, (*S*)-fluoxetine; MA, *N*-desmethyldiltiazem; UPLC, ultraperformance liquid chromatography; LC, liquid chromatography; MS, mass spectroscopy; DBOMF, dibenzyloxymethylfluorescein; BOMR, benzylresorufin; EMOCC, 7-methoxy-4-trifluoromethylcoumarin; $CHCl_3$, chloroform; MeOH, methanol; DMSO, dimethyl sulfoxide; *m*-CPBA, *m*-chloroperbenzoic acid; KP_i, potassium phosphate buffer; ACN, acetonitrile; (*S*)-FLXOH, (*S*)-*N*-hydroxyfluoxetine; MAOH, *N*-hydroxy-*N*-desmethyldiltiazem; DDES, *N*-desmethyldesipramine; (*S*)-NFLX, (*S*)-norfluoxetine; MD, *N,N*-didesmethyldiltiazem; DESOH, *N*-hydroxydesipramine; HLM, human liver microsome.

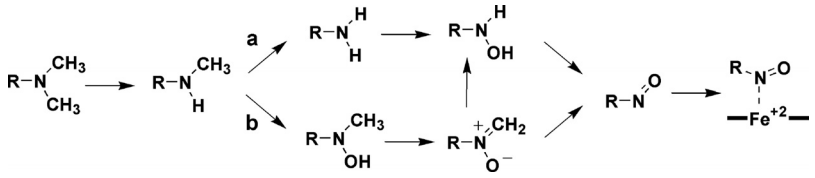

FIG. 1. Metabolism of alkyl amines by cytochrome P450 enzymes to MI complexes. Metabolism of these secondary amines leads to two primary metabolites: a primary amine (pathway a) and a secondary hydroxylamine (pathway b), both of which may contribute to MI complex formation. Secondary branching of the nitrone has been suggested (Jeffery and Mannering, 1983; Cerny and Hanzlik, 2005).

cause MI complex formation in microsomes or single enzyme systems (Jeffery and Mannering, 1983; Polasek and Miners, 2008; Zhang et al., 2009a).

The reaction sequence to MI complex is characterized by a major metabolic branch point, namely oxidation of the secondary amine to the primary amine via *N*-dealkylation (Fig. 1, pathway a) or to the secondary hydroxylamine by *N*-hydroxylation (Fig. 1, pathway b). P450-catalyzed *N*-dealkylation has been studied extensively; however, *N*-hydroxylation has received less attention. In addition, it is clear that both products are formed from a single substrate by multiple enzymes, which suggests that *N*-hydroxylation may be common (Baba et al., 1988).

A survey of the results of microsomal studies indicates that the relative rates of MI complex formation from intermediates tend to rank in the order primary hydroxylamine > nitrone > secondary hydroxylamine > secondary amine ≫ primary amine (Gumbrecht and Franklin, 1979; Jönsson and Lindeke, 1992; Bensoussan et al., 1995). The primary amine pathway (Fig. 1, pathway a) is often cited as the major pathway to MI complex from alkyl amines (Correia and Ortiz de Montellano, 2005). The conversion of primary amines to MI complexes has received considerable attention in which the slow step is thought to be *N*-hydroxylation of the primary amine (Buening and Franklin, 1976). However, the rate of MI complex formation from primary amines is significantly slower than the rate observed from the corresponding secondary amines. For example, Lindeke et al. (1979) studied the intermediates to MI complex formation during the metabolism of methamphetamine. They concluded that the secondary hydroxylamine pathway (Fig. 1, pathway b) is largely responsible for the formation of an MI complex in rat liver microsomes. It is reasonable to expect that the relative contributions of these two pathways to MI complex formation will depend on a number of factors including the enzyme-substrate pair, the amount and stability of the metabolites formed, and the effects of other enzymes on the generation of pathway intermediates in the systems of interest.

The relative importance of the two pathways from the secondary amines on the rate of MI complex formation in single enzyme systems has not been reported previously. This report addresses this gap by studying the metabolism of three secondary alkyl amines, each paired with a different P450 enzyme (Fig. 2). The enzyme-substrate pairs are DES with rat CYP2C11, (*S*)-FLX with human CYP2C19, and MA with human CYP3A4. In agreement with the proposal of Lindeke et al. (1979), we show that the secondary hydroxylamine pathway controls the rate of MI complex formation from secondary amines. In addition, we demonstrate that primary amine metabolites can accumulate to concentrations that will significantly inhibit MI complex formation by secondary amines.

Materials and Methods

Chemicals. All chemicals from commercial sources were of analytical grade. Solvents for Waters ACQUITY UPLC were LC-MS Optima grade. Human CYP3A4, rat CYP2C11, and human CYP2C19 Supersomes, coexpressed with cytochrome b_5 and cytochrome P450 reductase, were purchased from BD Biosciences (San Jose, CA). Desipramine, (*S*)-fluoxetine, and diltiazem were purchased from Sigma-Aldrich (St. Louis, MO). The internal standard, ring-labeled desipramine-d_4, was purchased from Cambridge Isotope Laboratories, Inc. (Andover, MA). The internal standards, fluoxetine-d_6 and norfluoxetine-d_6, were purchased from Cerilliant Corporation (Round Rock, TX). The fluorescent probe substrates and metabolites DBOMF (Vivid Green), BOMR (Vivid Red), EMOCC (Vivid Blue), fluorescein (DBOMF metabolite), and 7-hydroxy-4-trimethylcoumarin (EMOCC metabolite) were purchased from Invitrogen (Carlsbad, CA). Resorufin was purchased from Sigma-Aldrich. All other chemicals were purchased from Sigma-Aldrich unless specified.

Chemical Syntheses of Primary Amine and Secondary Hydroxylamine Metabolites and Deuterated Internal Standards of DES, (*S*)-FLX, and MA. *Preparation of deuterated 5-[3-aminopropyl]iminodibenzyl (desmethyldesipramine-d_4).* A solution of *N*-desmethyldesipramine (0.504 g, 2.00 mmol) in 10% DCl-D_2O (15 ml) was heated at 80°C for 8 h in a nitrogen-filled sealed heavy glass tube, according to the method reported previously (Baba et al., 1988). The reaction mixture was then cooled and adjusted to pH 10 with aqueous 2 N NaOH at 0°C and extracted with ether (three 100-ml washes). The combined extracts were washed with saturated NaCl solution and dried over Na_2SO_4. After evaporation of solvent under reduced pressure, the crude product was chromatographed on silica gel eluting with $CHCl_3$ and a $CHCl_3$-MeOH gradient to afford 0.416 g (82%) of desmethyldesipramine-d_4, as a thick gum. ^{1}H NMR (free base, 500 MHz) $CDCl_3$ δ: 1.75 (quintet, 2H, J = 7 Hz, –N–CH_2–CH_2–CH_2–N–), 2.76 (t, 2H, J = 7 Hz, –N–CH_2–CH_2–CH_2–N–), 3.17 (s, 4H, Ar–CH_2–CH_2–Ar), 3.80 (t, 2H, J = 6.5 Hz, Ar–N–CH_2–), 7.11–7.14 (m, 4H, ArH); MS [MH^+] 257.1 ($C_{17}H_{16}D_4N_2$ requires 256.3).

Preparation of deuterated 5-[3-(N-hydroxyl-N-methylamino)propyl]iminodibenzyl (N-hydroxydesipramine-d_4). An aqueous formaldehyde solution (37%, 90.6 mg, 3.02 mmol) was added to a solution of ring-deuterated 5-[3-(*N*-hydroxylaminopropyl]iminodibenzyl (330 mg, 1.2 mmol) in benzene (35 ml), and the reaction mixture was refluxed for 9 h with a Dean-Stark apparatus until no more water was collected. After evaporation of solvent, the crude product was purified by flash chromatography on silica gel, eluting with a hexane-ethyl acetate gradient to give 0.245 g (71%) of the deuterated *N*-methylene nitrone as a pale yellow oil. A stirred solution of deuterated *N*-methylene nitrone (0.150 g, 0.52 mmol) in MeOH (10 ml) was cooled to −10°C, and the reaction mixture was adjusted to pH 4 with 1 N HCl. Sodium cyanoborohydride (82.6 mg, 1.3 mmol) was added to the reaction at −10°C. The mixture was warmed to room temperature and stirred for 9 h. The reaction mixture was quenched by addition of 1 N HCl (1 ml), and the MeOH was

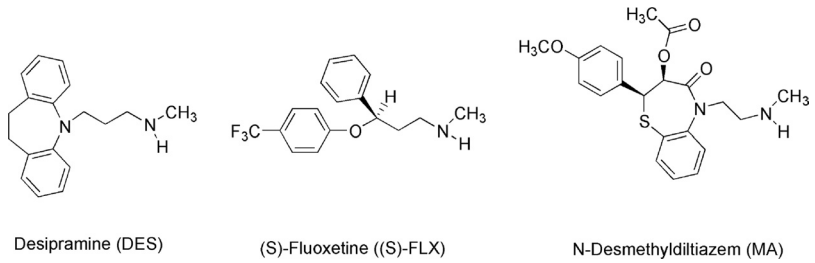

FIG. 2. Chemical structures of the three alkyl amine drugs used in this study.

removed under reduced pressure. The residue was dissolved in water (10 ml), made alkaline (pH 10) with 2 N NaOH solution, and then extracted with ether (three 40-ml washes). The combined organic extracts were washed with saturated NaCl solution and dried (Na_2SO_4). Evaporation of the solvent gave the crude product, which was purified by silica gel flash column chromatography eluting with $CHCl_3$ followed by a $CHCl_3$-MeOH gradient, which afforded 0.125 g (83%) of a thick liquid product, which was converted to its oxalic acid salt, obtained as a white solid, m.p. 121°C. The nondeuterated compound has been reported (Beckett et al., 1983). ^{1}H NMR (free base) (500 MHz) $CDCl_3$ δ: 1.86 (quintet, 2H, J = 7 Hz, –N–CH_2–CH_2–CH_2–N–), 2.59 (s, 3H, –N–CH_3), 2.72 (t, 2H, J = 7 Hz, –N–CH_2–CH_2–CH_2–N–), 3.17 (s, 4H, Ar–CH_2–CH_2–Ar), 3.82 (t, 2H, J = 6.5 Hz, Ar–N–CH_2–), 6.92–6.96 (m, 1H, ArH), 7.06–7.16 (m, 2H, ArH); MS [MH^+] 287 (d_4) (70), 288.4 (100), 289 (94), 290 (55) ($C_{18}H_{18}D_4N_2O$ requires 286.2).

Preparation of 5-[3-(N-trideuteromethylamino)propyl]iminodibenzyl (desipramine-methyl-d_3). A solution of 5-(3-chloropropyl)iminodibenzyl (0.160 g, 0.59 mmol) in MeOH (10 ml) in a 60-ml sealed heavy glass tube was cooled to 0°C. Methylamine-d_3 hydrochloride (Cambridge Isotope Laboratories) (0.125 g, 1.77 mmol) was added at 0°C followed by an aqueous solution of sodium carbonate (0.250 g, 2.3 mmol in 2 ml of water). The reaction mixture was saturated with N_2 gas, sealed, and heated at 110°C for 14 h. After cooling the pressure vessel tube at 0°C over 4 h, it was opened, and the MeOH was evaporated under reduced pressure. Water (10 ml) was added, and the mixture was extracted with $CHCl_3$ (three 15-ml washes). The combined organic extracts were washed with water and saturated NaCl solution and then dried (Na_2SO_4). Evaporation of solvent gave the crude product, which was purified by flash column chromatography on silica gel eluting with $CHCl_3$ followed by a $CHCl_3$-MeOH gradient, afforded 0.137 g (86%) of the desipramine-d_3, obtained as a thick gummy liquid. ^{1}H NMR (300 MHz) $CDCl_3$ δ: 1.91 (m, 2H, –N–CH_2–CH_2–CH_2–N–), 2.75 (t, 2H, J = 7.2 Hz, –N–CH_2–CH_2–CH_2–N–), 3.17 (s, 4H, Ar–CH_2–CH_2–Ar), 3.84 (t, 2H, J = 6.6 Hz, Ar–N–CH_2–), 6.93 (dt, 2H, ArH), 7.07–7.16 (m, 6H, ArH); MS [MH^+] 270.1 ($C_{18}H_{19}D_3N_2$ requires 269.2).

Preparation of (S)-fluoxetine and (S)-norfluoxetine. The (*S*)-enantiomers of fluoxetine and norfluoxetine were prepared from commercially available (*S*)-3-chloro-1-phenylpropanol by conversion to the corresponding 3-iodo compound and subsequent displacement with ammonia or methylamine, respectively (Corey and Reichard, 1989). Subsequent *O*-arylation of 4-chlorotrifluoromethylbenzene was accomplished using sodium hydride in DMSO (norfluoxetine) (Mitchell and Koening, 1995) or in dimethylacetamide (fluoxetine) (Kamal et al., 2002). The tartrate salts of norfluoxetine enantiomers were prepared by the method described previously (Hilborn et al., 2001).

Preparation of diltiazem-d_3. To a stirred solution of diltiazem (0.650 g, 1.44 mmol) in ethanol (195 ml) was added 13 ml of aqueous 5% NaOH. The resulting clear solution was stirred for 26 h at room temperature. The reaction mixture was then neutralized with cold aqueous 10% HCl, the solvents were removed under reduced pressure, and the residue was treated with aqueous 5% NaOH and extracted with $CHCl_3$ (three 30-ml washes). The combined organic extracts were washed with water and brine and then dried (Na_2SO_4). Removal of solvent gave crude product that was purified by flash column chromatography on silica gel eluting with $CHCl_3$, affording 0.530 g (98%) of *O*-desacetyldiltiazem as thick liquid. ^{1}H NMR (300 MHz) $CDCl_3$ δ: 2.69 [s, 6H, –N(CH_3)$_2$], 2.92–3.10 (m, 1H, –CH_2–NH–CH_3), 3.18–3.30 (m, 1H, –CH_2–NH–CH_3), 3.84 (s, 3H, –OCH_3), 4.18–4.25 (m, 1H, –CO–N–CH_2–), 4.30–4.39 (m, 1H, –CO–N–CH_2–), 4.61–4.72 (m, 1H, –CH–OH), 4.92 (d, 1H, J = 7.5 Hz, –S–CH–), 6.89–6.94 (m, 2H, ArH), 7.30–7.39 (m, 3H, ArH), 7.45 (dd, 1H, J = 1.5 and 7.1 Hz, ArH), 7.56 (ddd, 1H, J = 1.5 and 7.2 Hz, ArH), 7.72 (dd, 1H, J = 1.5 and 7.5 Hz, ArH); MS [MH^+] 373.3 ($C_{20}H_{24}N_2O_3S$ requires 372.3).

The intermediate *O*-desacetyldiltiazem (0.600 g, 1.61 mmol) was dissolved in CH_2Cl_2 (50 ml). Acetic anhydride-d_6 (0.885 g, 8.19 mmol) and 4-*N,N*-dimethylaminopyridine (0.426 g, 3.49 mmol) were added. The reaction mixture was stirred for 24 h at room temperature and then heated at reflux for 2 h. The solvent was then evaporated under reduced pressure, and the thick liquid obtained was purified by flash column chromatography on silica gel eluting with $CHCl_3$ to give 0.662 g (98%) of diltiazem-d_3 as a thick liquid, which was converted into its oxalic acid salt, obtained as a white solid, m.p. 150–151°C. ^{1}H NMR (300 MHz) CD_3OD δ: 2.98 [s, 6H, –N–(CH_3)$_2$], 3.32–3.41 (m, 1H, –CH_2–NH–CH_3), 3.59–3.68 (m, 1H, –CH_2–NH–CH_3), 3.83 (s, 3H, –OCH_3), 4.17–4.27 (m, 1H, –CO–N–CH_2–), 4.45–4.52 (m, 1H, –CO–N–CH_2–), 5.09 (d, 2H, J = 7.8 Hz, –CH–O–$COCD_3$ and –S–CH–), 6.88 (d, 2H, J = 8.7 Hz, ArH), 7.41–7.47 (m, 3H, ArH), 7.62–7.67 (m, 2H, ArH), 7.80 (d, 1H, J = 8.1 Hz, ArH); MS [MH^+] 418.3 ($C_{22}H_{23}D_3N_2O_4S$ requires 417.2).

Preparation of N-desmethyldiltiazem-d_3. Diltiazem was *N*-demethylated according to a method described previously (Alexander, 1993). In brief, diltiazem-d_3 (0.600 g, 1.15 mmol free base) was refluxed with α-chloroethyl chloroformate (0.365 g, 2.75 mmol) in 20 ml of 1,2-dichloroethane for 12 h. Solvent and α-chloroethyl chloroformate were evaporated under reduced pressure to obtain the carbamate ester. This ester was dissolved in 20 ml of MeOH and refluxed for 2 h. After evaporation of the MeOH, the gummy mass obtained was dissolved in a mixture of ethyl acetate-ether (1:1, 30 ml) and allowed to stand for 30 min. The resultant white solid was filtered, washed with ether, dried, and crystallized from EtOAc to afford 0.514 g (89%) of *N*-desmethyldiltiazem-d_3 HCl as a white solid, m.p. 133°C. ^{1}H NMR (500 MHz) $CDCl_3$ δ: 2.81 (t, 3H, J = 5.0 Hz, –CH_2–N–CH_3), 3.37–3.48 (m, 1H, –CH_2–*N*–CH_3), 3.51–3.57 (m, 1H, –CH_2–NH–CH_3), 3.86 (s, 3H, –OCH_3), 4.34–4.46 (m, 2H, –CO–N–CH_2–), 5.04 (d, 1H, J = 7.5 Hz, –CH–O–$COCD_3$), 5.11 (d, 1H, J = 7.5 Hz, –*S*–CH–), 6.93 (d, 2H, J = 9.0 Hz, ArH), 7.31–7.36 (m, 1H, ArH), 7.40 (d, 2H, J = 8.5 Hz, ArH), 7.59 (d, 2H, J = 4.0 Hz, ArH), 7.74 (d, 1H, J = 8.0 Hz, ArH), 9.53 (bs, 1H, –NH, exchangeable with D_2O); MS [MH^+] 404.2 ($C_{21}H_{21}D_3N_2O_4S$ requires 403.2).

Preparation of N-hydroxydesipramine oxalate. To a stirred solution of desipramine (free base, 0.500 g, 1.87 mmol) in MeOH (15 ml), acrylonitrile (0.5 g, 9.4 mmol) was added. The resulting solution was stirred for 24 to 32 h at room temperature. After the MeOH was evaporated, the resultant gummy mass was purified by flash chromatography on silica gel eluting with $CHCl_3$ to yield 0.540 g (90%) of the *N*-cyanoethyl intermediate as a thick gummy liquid. ^{1}H NMR (300 MHz) $CDCl_3$ δ: 1.95 (m, 2H, –N–CH_2–CH_2–CH_2–N–), 2.40 (s, 3H, –N–CH_3), 2.69–2.77 (m, 4H, –N–CH_2–CH_2–CN), 2.88 (t, 2H, J = 6.9 Hz, –N–CH_2–CH_2–CH_2–N–), 3.17 (s, 4H, Ar–CH_2–CH_2–Ar), 3.85 (t, 2H, J = 6.6 Hz, Ar–N–CH_2–), 6.96 (broad dt, 2H, ArH), 7.07–7.19 (m, 6H, ArH); MS [MH^+] 320.2 ($C_{21}H_{25}N_3$ requires 319.2).

A stirred solution of *N*-cyanoethyldesipramine (0.502 g, 1.57 mmol) in dry CH_2Cl_2 (20 ml) was cooled to −78°C and *m*-CPBA (77%, 0.185 g, 0.828 mmol) was added. The reaction mixture was stirred for 24 h at −78°C under argon and then washed sequentially with ice-cold aqueous 10% K_2CO_3 solution (three 10-ml washes), water (three 10-ml washes), and saturated NaCl (three 10-ml washes) and dried (Na_2SO_4). Evaporation of solvent gave crude product, which was purified by silica gel flash column chromatography eluting with $CHCl_3$ followed by a $CHCl_3$-MeOH gradient to afford 0.327 g (74%) of *N*-hydroxydesipramine as a thick liquid. The product was converted to its oxalate salt, m.p. 121°C. ^{1}H NMR (oxalate salt) (300 MHz) CD_3OD δ: 2.02 (m, 2H, –N–CH_2–CH_2–CH_2–N–), 2.99 (s, 3H, –N–CH_3), 3.16 (s, 4H, Ar–CH_2–CH_2–Ar), 3.26–3.34 (m, 2H, –N–CH_2–CH_2–N–), 3.88 (t, 2H, J = 6.6 Hz, Ar–N–CH_2–), 6.91–6.96 (m, 2H, ArH), 7.10–7.19 (m, 6H, ArH); ^{1}H NMR (base) (500 MHz) $CDCl_3$ δ: 1.88 (q, 2H, J = 7.0 Hz, –N–CH_2–CH_2–CH_2–N–), 2.60 (s, 3H, *N*–CH_3) 3.18 (s, 4H, Ar–CH_2–CH_2–Ar), 2.75 [t, 2H, J = 7.0 Hz, –CH_2–N(OH)–], 3.82 (t, J = 7.0 Hz, Ar-N-CH_2–), 6.93–6.96 (m, 2H, ArH), 7.09–7.15 (m, 6H, ArH); MS [MH^+] 283.2 ($C_{18}H_{22}N_2O$ requires 282.2).

*Preparation of (*S*)-N-hydroxyfluoxetine.* To a stirred solution of (*S*)-fluoxetine (0.500 g, 1.61 mmol) in MeOH (15 ml) acrylonitrile (0.429 g, 8.05 mmol) was added, and the mixture was treated as described for the first step in the preparation of *N*-hydroxydesipramine. The intermediate (*S*)-*N*-cyanoethylfluoxetine (0.514 g, 88%) was obtained as a thick liquid. ^{1}H NMR (500 MHz) $CDCl_3$ δ: 1.99–2.19 (m, 1H, –CH–CH_2–CH_2–), 2.18–2.28 (m, 1H, –CH–CH_2–CH_2–), 2.35 (s, 3H, –N–CH_3), 2.46–2.60 (m, 3H, –N–CH_2–CH_2–CN), 2.65–2.81 (m, 3H, –CH_2–N(CH_3)–CH_2–CH_2–CN), 5.41 (dd, 1H, J = 4.5 and 8.0 Hz, Ph–CH–CH_2–), 6.94 (d, 2H, J = 8.5 Hz, ArH), 7.30–7.40 (m, 5H, ArH), 7.45 (d, 2H, J = 8.5 Hz, ArH); MS [MH^+] 363.2 ($C_{20}H_{21}F_3N_2O$ requires 362.2).

The (*S*)-*N*-cyanoethylfluoxetine intermediate (0.300 g, 0.828 mmol) was treated with *m*-CPBA (77%, 0.185 g, 0.828 mmol) in dry CH_2Cl_2 at −78°C as described for the second step in the preparation of *N*-hydroxydesipramine. Workup and chromatography as described therein afforded 0.247 g (92%) of (*S*)-*N*-hydroxyfluoxetine as a thick gummy liquid. ^{1}H NMR (500 MHz) $CDCl_3$ δ: 2.14–2.21 (m, 1H, –CH–CH_2–CH_2–), 2.28–2.36 (m, 1H, –CH–CH_2–CH_2–), 2.67

(s, 3H, –N–CH_3), 2.78–2.85 (m, 2H, –CH_2–N(OH)–CH_3), 5.34 (dd, 1H, J = 5 and 8.5 Hz, Ph–CH–CH_2–), 6.93 (d, 2H, J = 8.5 Hz, ArH), 7.29–7.37 (m, 5H, ArH), 7.45 (d, 2H, J = 8.5 Hz, ArH); MS [MH^+] 326.2 ($C_{17}H_{18}F_3NO_2$ requires 325.1).

Preparation of N-hydroxyfluoxetine-d_5. To a stirred solution of fluoxetine-d_5 (phenyl-d_5) (0.100 g, 0.32 mmol) (C/D/N Isotopes Inc., Pointe-Claire, QC, Canada) in MeOH (15 ml) was added acrylonitrile (0.168 g, 3.2 mmol). The mixture was treated as described for the first step in the preparation of *N*-hydroxydesipramine. The intermediate *N*-cyanoethylfluoxetine-d_5 (0.110 g, 94%) was obtained as a thick gum. ^{1}H NMR (500 MHz) $CDCl_3$ δ: 1.98–2.12 (m, 1H, –CH–CH_2–CH_2–), 2.18–2.28 (m, 1H, –CH–CH_2–CH_2–), 2.35 (s, 3H, –N–CH_3), 2.47–2.60 (m, 2H, –CH_2–CN), 2.65–2.83 [m, 4H, –CH_2–N(CH_3)–CH_2–CH_2–CN], 5.41 (dd, 1H, J = 4.5 and 8.0 Hz, Ph–CH–CH_2–), 6.94 (d, 2H, J = 8.5 Hz, ArH), 7.45(d, 2H, J = 8.5 Hz, ArH); MS [MH^+] 368.3 ($C_{20}H_{26}F_3N_2O$, requires 367.2).

The *N*-cyanoethylfluoxetine-d_5 intermediate (0.100 g, 0.272 mmol) was treated with *m*-CPBA (77%, 61 mg, 0.272 mmol) in dry CH_2Cl_2 at −78°C and further treated as described for the second step in the preparation of *N*-hydroxydesipramine. Workup and chromatography as described therein afforded *N*-hydroxyfluoxetine-d_5 (83 mg, 92%) as a thick gum. ^{1}H NMR (500 MHz) $CDCl_3$ δ: 2.14–2.22 (m, 1H, –CH–CH_2–CH_2–), 2.27–2.37 (m, 1H, –CH–CH_2–CH_2–), 2.68 (s, 3H, –NH–CH_3), 2.78–2.81 [m, 2H, –CH_2–N(OH)–CH_3], 5.31 (m, 1H, Ph–CH–CH_2–), 6.92 (d, 2H, J = 8.0 Hz, ArH), 7.45 (d, 2H, J = 8.5 Hz, ArH); MS [MH^+] 331.3 ($C_{17}H_{18}D_5F_3NO_2$ requires 330.2).

Preparation of N-hydroxy-N-desmethyldiltiazem oxalate. To a stirred solution of *N*-desmethyldiltiazem (0.458 g, 1.14 mmol) in MeOH (15 ml) was added acrylonitrile (0.303 g, 5.72 mmol). The mixture was treated as described for the first step in the preparation of *N*-hydroxydesipramine. The intermediate *N*-cyanoethyl-*N*-desmethyldiltiazem (0.488 g, 94%) was obtained as a thick liquid. ^{1}H NMR (300 MHz) $CDCl_3$ δ: 1.92 (s, 3H, –$COCH_3$), 2.37 (s, 3H, –N–CH_3), 2.45–2.88 (m, 6H, H_3C–N–CH_2–CH_2–CN and –CH_2–N–CH_3), 3.84 (s, 3H, –OCH_3), 4.28–4.37 (m, 1H, –CO–N–CH_2–), 4.77–4.80 (m, 1H, –CO–N–CH_2–), 5.01 (d, 1H, J = 7.8 Hz, –S–CH–), 5.14 (d, 1H, J = 7.8 Hz, –CH–O–$COCH_3$), 6.89–6.93 (m, 2H, ArH), 7.28–7.32 (m, 1H, ArH), 7.41–7.45 (m, 2H, ArH), 7.50–7.56 (m, 2H, ArH), 7.70–7.73 (m, 1H, ArH); MS [MH^+] 454.3 ($C_{24}H_{27}N_3O_4S$ requires 453.2).

The *N*-cyanoethyl-*N*-desmethyldiltiazem intermediate (0.250 g, 0.55 mmol) was mixed with *m*-CPBA (77%, 0.123 g, 0.55 mmol) in dry CH_2Cl_2 at −78°C and further treated as described for the second step in the preparation of *N*-hydroxydesipramine. Workup and chromatography as described therein afforded *N*-hydroxy-*N*-desmethyldiltiazem (0.193 g, 84%) as a thick liquid. The oxalic acid salt was obtained as a white solid, m.p. 145°C. ^{1}H NMR (300 MHz) CD_3OD δ: 1.88 (s, 3H, –$COCH_3$), 2.87 (s, 3H, –N–CH_3), 3.05–3.15 (m, 1H, –CH_2–N–CH_3), 3.36–3.43 (m, 1H, –CH_2–NH–CH_3), 3.82 (s, 3H, –OCH_3), 4.00–4.09 (m, 1H, –CO–N–CH_2), 4.46–4.55 (m, 1H, –CO–N–CH_2–), 5.09 (d, 2H, J = 7.8 Hz, –CH–O–$COCH_3$ and –S–CH–), 6.91–6.95 (m, 2H, ArH), 7.38–7.46 (m, 3H, ArH), 7.60–7.68 (m, 2H, ArH), 7.76–7.79 (m, 1H, ArH); MS [MH^+] 417.3 ($C_{21}H_{24}N_2O_5S$, requires 416.1).

Preparation of N-hydroxy-N-desmethyldiltiazem-d_3. To a stirred solution of *N*-desmethyldiltiazem-d_3 (0.330 g, 0.81 mmol) in MeOH (15 ml) was added acrylonitrile (43.4 mg, 5.72 mmol). The mixture was treated as described for the first step in the preparation of *N*-hydroxydesipramine. The intermediate *N*-cyanoethyl-*N*-desmethyldiltiazem-d_3 (0.340 g, 91%) was obtained as a thick liquid. ^{1}H NMR (500 MHz) $CDCl_3$ δ: 2.42–2.84 (m, 10H, –N–CH_2–CH_2–CN, –CH_2–N–CH_3, –CH_2–N–CH_3, and –CO–N–CH_2), 3.86 (s, 3H, –OCH_3), 4.30–4.45 (m, 1H, –CO –N–CH_2–), 5.04 (d, 1H, J = 7.5 Hz, –CH–O–$COCD_3$), 5.17 (d, 1H, J = 8.0 Hz, –S–CH–), 6.92 (d, 2H, J = 8.50 Hz, ArH), 7.31–7.35 (m, 2H, ArH), 7.43 (d, 2H, J = 8.5 Hz, ArH), 7.54 (d, 1H, J = 3.0 Hz, ArH), 7.73 (d, 1H, J = 7.5 Hz, ArH); MS [MH^+] 457.3 ($C_{24}H_{30}N_3O_4S$, requires 456.2).

The *N*-cyanoethyl-*N*-desmethyldiltiazem-d_3 intermediate (0.220 g, 0.48 mmol) was treated with *m*-CPBA (77%, 0.084 g, 0.48 mmol) in dry CH_2Cl_2 at −78°C as described for the second step in the preparation of *N*-hydroxydesipramine. Workup and chromatography as described therein afforded *N*-hydroxy-*N*-desmethyldiltiazem-d_3 (0.162 g, 81%) as a thick liquid. The oxalic acid salt was a white solid, m.p. 150–152°C. ^{1}H NMR (500 MHz) CD_3OD δ: 2.73 (s, 3H, –N–CH_3), 2.94 (m, 2H, –CH_2–N–CH_3), 3.71 (s, 3H, –OCH_3), 3.92 (m, 1H, –CO–N–CH_2–), 4.38 (m, 1H, –CO–N–CH_2–), 6.80 (m, 2H, ArH), 7.28–7.66 (m, 6H, ArH); MS [MH^+] 420.2 ($C_{21}H_{21}D_3N_2O_5S$ requires 419.2).

MI Complex Formation. The formation of MI complexes was monitored on an Olis-modernized Aminco DW-2 spectrophotometer (Olis, Bogart, GA). Sample and reference cuvettes contained 0.11 μM enzyme, 0.1 M KP_i buffer (pH = 7.4), and 10 μM secondary hydroxylamine, primary amine, or secondary amine to a total volume of 0.45 ml. After 3 min of preincubation at 37°C, NADPH (10 mM, 0.05 ml) and KP_i buffer (0.1 M, 0.05 ml) were added to the sample and reference cuvettes, respectively. The spectrophotometer was set to scan, repetitively, from 495 to 430 nm (5-nm intervals) until MI complex formation reached completion. The concentrations of MI complexes were estimated using 65 cm^{-1} mM^{-1}, the extinction coefficient for the absorbance difference between 490 and 455 nm (Liu and Franklin, 1985). Initial rates of enzyme inactivation and maximum absorbance were estimated by fitting the data to the standard monoexponential function $Abs_t = Abs_{max}(1 - e^{-kt})$, where k is equal to the initial rate of MI complex formation. After each MI complex formed to completion, quasi-reversibility was tested by adding potassium ferricyanide (100 mM, 5 μl) to the sample and reference cuvettes.

Stoichiometry of P450 Oxidation of the Secondary Amines. MI complex formation resulting from metabolism of the secondary amines by their respective P450 enzymes was monitored as described previously until the reactions were complete. For analysis of metabolite concentrations by LC-MS/MS [(*S*)-FLX and MA] or LC-MS (DES), aliquots were removed from the sample and reference cuvettes and added to an equal volume of ACN containing internal standards. The concentrations of alkyl amines and enzymes were DES or DES-d_3 (100 μM) and CYP2C11 (0.10 μM), (*S*)-FLX (10 μM) and CYP2C19 (0.10 μM), and MA (10 μM) and CYP3A4 (0.25 μM). The competitive isotope effect experiment incubations contained a mixture of equal concentrations (50 μM) of ring-deuterated DES (DES-d_4) and DES-d_3.

Cytochrome P450 Activity Assays. Dealkylation of fluorescent probe substrates BOMR, EMOCC, and DBOMF by CYP2C11, CYP2C19, and CYP3A4, respectively, was assayed fluorometrically (plate reader) using excitation and emission wavelengths as suggested by Invitrogen. The K_m value for each probe substrate-enzyme pair was determined (BOMR-CYP2C11 = 0.13 μM, EMOCC-CYP2C19 = 0.90 μM, and DBOMF-CYP3A4 = 1.5 μM). Substrate concentrations equal to the K_m values determined were used in assays for changes in enzyme activity in the TDI studies. Probe substrates were incubated for a time period that fell within the linear range of product formation: BOMR-2C11 15 min, EMOCC-2C19 8 min, and DBOMF-3A4 4 min.

Inhibition of MI Complex Formation Caused by Coincubation with the Primary Amines. Time-dependent inhibition of CYP2C11, CYP2C19, and CYP3A4 activity was assayed using a 96-well format. Each inactivation assay well contained 0.05 μM enzyme, 0.1 M KP_i buffer, and secondary alkyl amine substrate [50 μM DES, 10 μM (*S*)-FLX, or 2 μM MA] or secondary hydroxylamine substrate [1 μM DOH, 5 μM (*S*)-FLXOH, or 0.5 μM MAOH] alone or with the respective primary amine [1 μM DDES, 0.1 μM (*S*)-NFLX, or 0.2 μM MD]. Control wells, without inhibitor, were treated in the same manner. Inactivation was initiated by addition of NADPH (10 mM, 0.02 ml) after a 3-min equilibration period at 37°C. Aliquots (0.02 ml, 1:10 dilution of the inactivation assay) were removed from the inactivation assay wells at timed intervals (0.5, 1, 2, 4, and 7 min) and transferred to activity assay wells to determine enzyme activity. The activity assay wells contained KP_i buffer (0.1 M), NADPH (1 mM), and the appropriate concentration of probe substrate. The activity assay wells were incubated over the appropriate time interval and were quenched with 0.1 ml of isopropanol. The contents of the activity assay wells were then transferred to a second 96-well plate and fluorescent metabolite concentrations were determined using a Microplate Spectrophotometer Gemini XPS (Molecular Devices, Sunnyvale, CA). Rates of enzyme inactivation were estimated from the slopes of the semilog plots of percent remaining enzyme activity in the presence and absence of inactivator with time.

LC-MS and LC-MS/MS Methods. Synthetic and stable-labeled internal standards for substrates and metabolites were used to develop LC methods, to optimize MS conditions, and to identify new metabolites [(*S*)-FLXOH and MAOH].

DES-related assays. LC-MS analysis of the metabolites of DES, DESOH, and DDES was performed on a Micromass Platform LCZ (Waters, Milford, MA). The Micromass Platform LCZ, equipped with Shimadzu LC-10AD pumps and autoinjector (Shimadzu Scientific Instruments, Inc., Columbia, MD), was operated in the electrospray positive ion mode. Analyte separation

was achieved using a Zorbax SB-C_3 column (150 × 2.1 mm, 5 μm particle size) at a flow rate of 0.4 ml/min. Solvent A was Nanopure water with 0.025% acetic acid and 0.01% *n*-propylamine. Solvent B was HPLC-grade ACN with 0.025% acetic acid and 0.01% *n*-propylamine. The solvent program was 70% A:30% B (0–0.5 min), linear gradient to 40% B (0.5–3.5 min), and linear gradient to 80% B (3.5–6 min), which was held constant from 6 to 7 min. The total run time was 12 min. The retention times were 5.2 and 7.2 min for DDES (MH^+: *m/z* = 253.3 d_0 and *m/z* = 256.3 d_3 substrates) and DESOH (MH^+: *m/z* = 283.3 d_0 and *m/z* = 286.3 d_3 substrate), respectively. For quantification, standard curves were constructed using ring-labeled (DES-d_4, DDES-d_4, and DESOH-d_4) internal standards. Data were acquired in the SIM mode, and peak areas were corrected for ion overlap as required. The cone voltage was 25 V for all DES-related compounds. In the competitive isotope effect experiments, peak area ratios of DESOH and DDES metabolites for coincubated ring-labeled DES-d_4 and DES-d_3 were corrected for measured substrate concentrations and ion overlap based on the ion envelopes of the substrates as necessary.

All other incubation samples were analyzed for metabolites using a Micromass Premier XE (Waters) equipped with an ACQUITY UPLC system and an autoinjector integral to the ACQUITY UPLC system. Chromatographic separations were achieved on an ACQUITY UPLC C_{18} BEH column (2.1 × 50 mm, 1.7 μm; Waters). The mass spectrometer was operated in the positive ion mode.

(S)-FLX-related assays. These substrates and metabolites were separated using a linear gradient at 0.3 ml/min and mobile phases A (0.1% formic acid in water) and B (0.1% formic acid in ACN). The gradient started at 90% A (0–0.5 min). Solvent B was linearly increased from 10% at 0.5 min to 100% at 4 min. The total run time was 5 min. The parent and product ions monitored for (*S*)-FLX were 310 > 44 *m/z*, for (*S*)-NFLX were 296 > 134 *m/z*, and for (*S*)-FLXOH were 326 > 60 *m/z*. The parent and product ions for internal standards were FLX-d_6 316 > 44 *m/z*, NFLX-d_6 302 > 140 *m/z*, and FLXOH-d_5 331 > 60 *m/z*. The cone and collision energies for (*S*)-FLX and FLX-d_6 were 20 V and 15 kV, for (*S*)-NFLX and NFLX-d_6 were 10 V and 5 kV, and for (*S*)-FLXOH and FLXOH-d_5 were 12 V and 10 kV.

MA-related assays. These compounds were separated using a linear gradient at 0.3 ml/min and mobile phases A (0.1% formic acid in water) and B (0.1% formic acid in ACN). The gradient started with 80% A (0–0.5 min). Solvent B was linearly increased to 100% over 3.5 min and held constant at 100% for 0.5 min. The total run time was 5.5 min. The parent and product ions monitored for MA were 401 > 178 *m/z*, for MD were 387 > 178 *m/z*, and for MAOH were 416 > 178 *m/z*. Internal standards for MA-d_3 were 404 > 178 *m/z*, for MAOH-d_3 were 419 > 178 *m/z*, and for alprazolam were 309 > 205 *m/z*. The cone and collision energies for MA and MA-d_3 were 25 V and 25 kV, for MAOH and MAOH-d_3 were 30 V and 20 kV, for MD were 25 V and 25 kV, and for alprazolam were 30 V and 35 kV.

Results

Synthesis of Metabolites and Internal Standards. The structures of the secondary amines used in this study are given in Fig. 2. Synthesis of the secondary hydroxylamines from the corresponding secondary amines was accomplished by the method of O'Neil et al. (2001), in which *N*-alkylation of the secondary amine with acrylonitrile is followed by *N*-oxidation with *m*-CPBA and Cope elimination of the protecting group. (*S*)-FLXOH and MAOH have not been reported previously. DESOH and MAOH were prepared as the oxalate salts. Stable-labeled standards of the substrates and metabolites were prepared or purchased, with the exception of MD. DDES-d_4 was obtained by acid-catalyzed exchange of four or more deuterium atoms in the aromatic rings by the method of Baba et al. (1988). DESOH-d_4 was synthesized from deuterated imidodibenzyl-d_4, exchanged by the same method. DES-d_3, labeled on the *N*-methyl carbon, was synthesized by reaction of trideuteromethylamine with 3-chloroimidodibenzylpropane. FLX-d_6 and NFLX-d_6 were purchased, and FLXOH-d_5 was prepared from commercially available FLX-d_5. Internal standards MA-d_3 and MAOH-d_3,with three deuterium atoms in the acetoxy methyl group, were synthesized.

MI Complex Formation. MI complexes were observed upon incubation of the three secondary amines, DES, (*S*)-FLX, and MA, and by their respective major metabolites in the presence of CYP2C11, CYP2C19, and CYP3A4. Representative spectra obtained for the secondary amines, secondary hydroxylamines, and primary amines are shown in Fig. 3. The absorbance maxima (λ_{max}) were DES, DDES, DOH-CYP2C11 (λ_{max} = 455 nm), (*S*)-FLX, (*S*)-NFLX, and (*S*)-FLXOH-CYP2C19 (λ_{max} = 458 nm). In the MA-CYP3A4 series, the tentative MI complex spectrum of MD was red-shifted (λ_{max} = 460 nm) and asymmetric compared with the spectra for MA and MAOH (λ_{max} = 452 nm). The theoretical concentrations of the MI complexes were calculated based on the literature extinction coefficient of 65 mM^{-1} cm^{-1} for the 455 to 490 nm absorbance difference (Liu and Franklin, 1985). The P450 concentrations provided by BD Gentest were confirmed by CO difference spectra and then were used to calculate the theoretical yield of MI complex. The concentrations of the MI complexes from incubations with the secondary hydroxylamines were 100, 98, and 115% of theoretical for DESOH, (*S*)-FLXOH, and MAOH, respectively. The corresponding values for the secondary amines were 80, 90, and 118% of theoretical values, whereas the values for the primary amines were much lower (11, 8, and 23%, respectively). After each MI complex formed to completion for each inhibitor-enzyme pair, potassium ferricyanide was added to

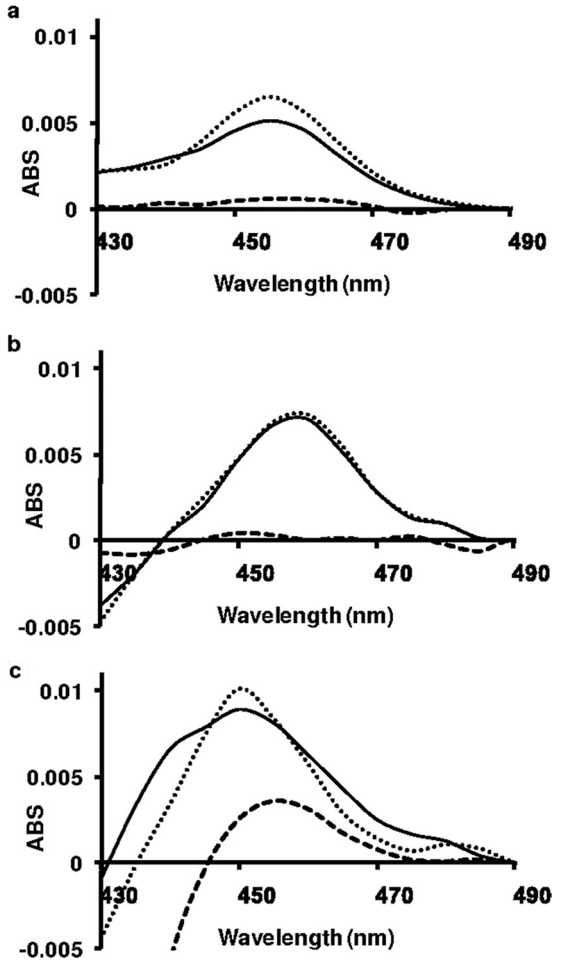

FIG. 3. Final MI complex spectra obtained by incubation of each compound at a concentration 10 μM. a, DES series incubated with CYP2C11. b, FLX series incubated with CYP2C19. c, MA series incubated with CYP3A4. MI complex formation by each secondary amine (——), primary amine(– – –), and secondary hydroxylamine (· · · · ·). The absorption (ABS) maximum for each complex ranged from 452 to 460 nm. Scans were recorded for 15 min total (20-s intervals). After MI complex formation with each inhibitor-enzyme pair was complete, the potassium ferricyanide reversal test was used. In each case, loss of peak at approximately 455 nm was observed after addition of potassium ferricyanide.

the sample and reference cuvettes to test for quasi-reversibility of the MI complex. In each case, loss of the peak at approximately 455 nm was observed.

The accumulation of MI complexes from these alkyl amines and metabolites are shown in Fig. 4. In each series, MI complex formation rates for the secondary amines were markedly faster than from the primary amines but noticeably slower than the rates observed from the secondary hydroxylamines. MI complex formation from the primary amines, DDES and (*S*)-NFLX, was barely discernable and incomplete (11 and 8% of the theoretical yield, respectively). For incubations of MD with CYP3A4, a rapid burst in absorbance at 460 nm was observed in the first two scans, which accounted for 18% of theoretical yield, followed by a gradual increase to 23% of theoretical yield by 15 min. This unusual biphasic accumulation profile could result from a contaminant present in the primary amine MD; however, identical results were obtained with a sample of MD purified by semipreparative HPLC. Overall, the relative rates of MI complex formation follow the consistent order secondary hydroxylamine > secondary amine ≫ primary amine.

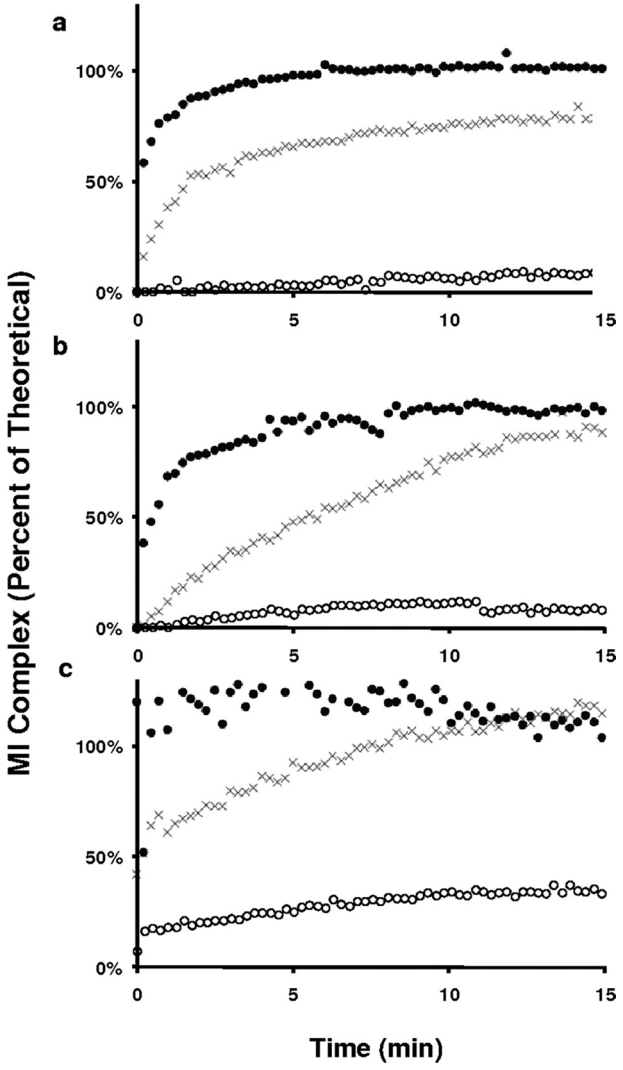

FIG. 4. The accumulation of MI complexes by secondary amines (X), primary amines (○), and secondary hydroxylamines (●). a, DES series. b, FLX series. c, MA series. The theoretical concentration of MI complex was calculated based on total P450 enzyme using the molar extinct coefficient of 65 mM^{-1} cm^{-1} (Liu and Franklin, 1985).

Stoichiometry of P450 Oxidation of the Secondary Amines. The product stoichiometry of the P450-catalyzed oxidation of the secondary amines was determined from the concentrations of the corresponding primary amine and secondary hydroxylamine metabolites and MI complexes (Table 1). The concentrations of the alkyl amines and P450s used in these experiments are in the legend to Table 1. Metabolites were quantitated by LC-MS or LC-MS/MS using authentic standards, and standard curves were constructed using stable-labeled internal standards or, in the case of MD, alprazolam. The primary and secondary amines were stable in solution during the sample workup and subsequent analysis. Stable-labeled internal standards were used for quantitation of the secondary hydroxylamines because of concerns of stability through sample workup and analysis. Structure assignments for the metabolites were made by comparison to the mass spectra and retention times of authentic standards obtained from commercial sources (DDES, NFLX, and MD) or by synthesis [DESOH, (*S*)-NFLXOH, and MAOH].

Metabolite formation was NADPH-dependent and negligible amounts of the metabolites were observed in control incubations. From each substrate, the primary amine and the secondary hydroxylamine metabolites were observed, and the primary amine was the major metabolite. The MI complexes accounted for 7, 17, and 37% of total products from DES-CYP2C11, (*S*)-FLX-CYP2C19, and MA-CYP3A4, respectively. The ratio of metabolites (primary amine/secondary hydroxylamine) (Table 1) observed ranged from 2.4:1 (MA-CYP3A4) to 17:1 [(*S*)-FLX-CYP2C19].

A second branching ratio [primary amine/(secondary hydroxylamine + MI complex)] (Table 1) was also calculated. The branching ratio is particularly meaningful if further metabolism of the secondary hydroxylamines, rather than the primary amines, leads to MI complex formation because it provides an improved estimate of the true ratio of the rates of *N*-dealkylation to *N*-hydroxylation. The calculated ratios ranged from 0.80:1 (MA-CYP3A4) to 3.6:1 [(*S*)-FLX-CYP2C19]. Although the branching ratios are probably different from the "true" ratios of product formation rates, it seems likely from these data that secondary hydroxylamine formation from secondary amines may occasionally exceed rates of *N*-dealkylation.

TABLE 1

Final concentrations of primary metabolites and MI complexes formed from desipramine, (S)-fluoxetine, and N-desmethyldiltiazem

The concentrations of the three products, primary amine, secondary hydroxylamine, and MI complex, from incubations with 100 μM DES, 10 μM FLX, 10 μM MA, and 100 μM DES-d_3. The concentration of enzyme in each experiment was 0.10 μM, except for CYP3A4 for which the concentration was 0.25 μM. Numbers in parentheses are the S.D. of triplicate experiments or S.E. of the ratios.

Substrate/Enzyme	Primary Amine	Secondary Hydroxylamine	MI Complex	MR[a]	BR[b]
	μM	*μM*	*μM*		
Desipramine/CYP2C11	0.89 (0.10)	0.23 (0.01)	0.08 (0.01)	3.9 (0.5)	2.9 (0.4)
(*S*)-Fluoxetine/CYP2C19	0.50 (0.01)	0.030 (0.001)	0.11 (0.01)	17 (1)	3.6 (0.4)
N-Desmethyldiltiazem/CYP3A4	0.23 (0.02)	0.10 (0.01)	0.19 (0.01)	2.4 (0.3)	0.80 (0.09)
Desipramine-methyl-d_3/CYP2C11	0.40 (0.04)	0.27 (0.02)	0.07 (0.02)	1.5 (0.2)	1.2 (0.4)

[a] Metabolite ratio (MR): primary amine/secondary hydroxylamine.
[b] Branching ratio (BR): primary amine/(secondary hydroxylamine + MI complex).

The DES-CYP2C11 system was probed for isotope effects in *N*-dealkylation, *N*-hydroxylation, and MI complex formation by comparison of the product profiles from separate incubations with DES and DES-d_3. A significant normal isotope effect of 2.2 (0.3) was observed for final DDES concentrations, whereas an inverse isotope effect was observed for the concentrations of DOH [0.85 (0.07)]. The apparent isotope effect ratio for the concentrations of MI complex in the incubations was 1.1 (0.4). The calculated product ratios, although reflecting the effects of the underlying isotope effects, are not true kinetic isotope effects because they were not obtained at steady state.

The initial rates of MI complex formation for DES and DES-d_3 were estimated by fitting the progress curves to the function $Abs_t = Abs_{max}(1 - e^{-kt})$. The estimates of the initial rates of MI complex formation were not significantly different [k_{d0} = 0.40 (0.01) min^{-1} versus k_{d3} 0.44 (0.07) min^{-1}; $p > 0.05$, two-tailed t test], and the calculated isotope effect was slightly inverse [$^{H}k/^{D}k$ = 0.91 (0.10)], but not significantly different from 1.

In addition, we performed a competitive experiment with equal molar amounts of DES and DES-d_3. The DES used in this experiment was d_4 ring-labeled to distinguish the products of *N*-dealkylation from DES-d_3 and DES-d_0. The respective competitive isotope effects on product ratios were 1.8 (0.1) for *N*-demethylation (DDES) and 0.52 (0.01) for *N*-hydroxylation (DESOH).

These results compare favorably with those of a previous report, in which deuterium isotope effects and metabolic switching for the metabolism of cyclohexylamine to cyclohexanone and cyclohexylhydroxylamine in rabbit liver microsomes of ^{D}V = 1.75 C–H bond oxidation and ^{D}V = 0.85 for *N*-hydroxylation in steady-state experiments (Kurebayashi, 1989). Together, these metabolic switching results indicate that *N*-dealkylation and *N*-oxygenation probably arise from a common P450 cycle intermediate (Chunsen et al., 2009).

These studies provide insights into the metabolism of these secondary amine drugs with respect to MI complex formation. First, primary amines and secondary hydroxylamines are formed in significant quantities from each of these secondary alkyl amines. Second, the MI complex comprises a significant fraction of the total products measured, suggesting that the pathways to MI complex are efficient (low partition ratio). In the cases of (*S*)-FLX and MA metabolism, the final concentrations of the secondary hydroxylamines were less than the corresponding MI complexes (27 and 51%, respectively). These results imply that these secondary hydroxylamines have a high affinity for the enzymes and that the "slow step" in the secondary hydroxylamine pathway could be *N*-hydroxylation of the secondary amines.

The isotope effect experiments with DES provide additional insights. First, deuterium substitution at the *N*-methyl group of DES provided significant normal isotope effects in both the competitive and noncompetitive experiments. The inverse isotope effect in the competitive experiment demonstrates that metabolic switching occurs between *N*-dealkylation and *N*-hydroxylation. A more complete mechanistic interpretation of these results would require experiments in the steady state, as well as a consideration of the effects of subsequent isotope effects for further metabolism of the secondary hydroxylamine. Second, in the noncompetitive design, the isotope effects on DDES concentration were normal (2.2), whereas the isotope effects for initial MI complex formation rate and the final concentrations of DESOH and MI complex were not significantly different from 1. The lack of a significant isotope effect on the initial rate of complex formation indicates that the primary amine pathway must play a minor role in MI complex formation from DES.

Inhibition of MI Complex Formation by the Primary Amines. The rates of accumulation of MI complex in each series follow the general trend of secondary hydroxylamine > secondary amine ≫ primary amine (Fig. 3). The primary amines are the major metabolites observed and accumulate to significant concentrations in the incubations with the secondary amines [DDES = 0.89 μM with 0.10 μM 2C11; (*S*)-NFLX = 0.50 μM with 0.10 μM 2C19; and MD = 0.23 μM with 0.25 μM 3A4] (Table 1).

The primary amine metabolites, although poor inactivators of the enzymes, may serve as competitive inhibitors of MI complex formation by competing with the substrates and products of the secondary hydroxylamine pathway. The reversible K_i for inhibition of CYP3A4 activity by MD in HLMs is 0.2 μM (Zhao et al., 2007). The calculated I/K_i value based on the final concentration of MD in our incubations (0.23/0.2 μM) is approximately 1, suggesting that inhibition of inactivation may have occurred in our studies. Reversible K_i estimates were also determined for DDES-CYP2C11 (0.8 μM) and (*S*)-NFLX-CYP2C19 (0.3 μM) from which I/K_i values for the final concentrations of the primary amines of 1.1 and 1.6 can be calculated, respectively. Because these ratios are all near 1, it is likely that the primary amines will compete with substrates and other pathway metabolites for active enzyme and progressively slow the rates of enzyme inactivation.

To test for this possibility, we performed a series of studies to examine the effects of the primary amines on enzyme inactivation by both secondary amines and their secondary hydroxylamine metabolites. The concentrations of the secondary amines in the inactivation assays and estimates of reversible affinities for their respective enzymes were as follows: DES = 50 μM with CYP2C11 (IC_{50} = 5 μM, data not shown), (*S*)-FLX = 10 μM with CYP2C19 (IC_{50} = 4.7 μM in HLMs) (Di Marco et al., 2007), and MA = 2 μM with CYP3A4 (K_i = 2 μM in HLMs) (Zhao et al., 2007). The secondary hydroxylamine substrate concentrations used were lower to facilitate data acquisition and curve-fitting: DESOH = 1 μM, (*S*)-FLXOH = 5 μM, and MAOH = 0.5 μM. The initial rates of the loss of enzyme activity caused by the secondary amines and secondary hydroxylamines were determined in triplicate in the presence and absence of fixed concentrations of the primary amines at their respective K_i or IC_{50} values.

The results of these experiments are given in Fig. 5, which shows the initial rates of inactivation as a function of the inhibitor(s) in the inactivation assays. Inactivation caused by the secondary amines and secondary hydroxylamines were, in all cases, significantly ($p < 0.05$) inhibited by coincubation with the respective primary amines. Note that the concentrations of primary amines (*S*)-NFLX and MD required to inhibit inactivation by roughly 50% were less than their concentrations measured during formation of MI complexes caused by the secondary amines. These results show that the primary amine metabolites generated from the secondary amines will cause meaningful inhibition of the formation of MI complexes from the metabolism of the secondary amines (Fig. 6).

Discussion

The pathways of P450-catalyzed metabolism of the alkyl amine moiety include *N*-dealkylation and *N*-hydroxylation reactions that result in the formation of a catalytically inactive MI complex (Fig. 1). A significant number of DDIs are believed to arise from the formation of MI complexes by alkyl amine-containing drugs (Backman et al., 1994; Mayhew et al., 2000; Hall et al., 2003; Zhang et al., 2010). Considerable effort has been directed toward development of a model to predict the magnitude of DDIs using in vitro data. Mayhew et al. (2000) developed a model to account for interactions caused by fluoxetine, *N*-desmethyldiltiazem, and clarithromycin with CYP3A. This model assumed a hyperbolic relationship between alkyl amine concentration and MI complex formation rates in vitro and in vivo. The original model was subsequently modified to better predict the magnitude of interactions in the liver and gut and to account for the

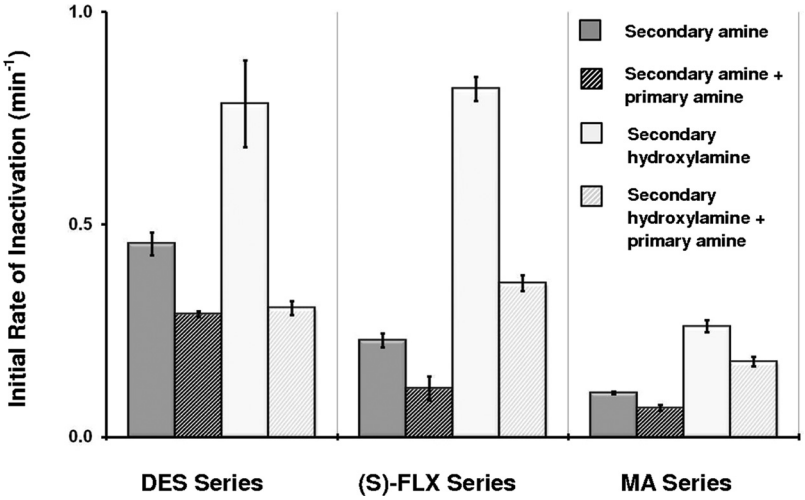

FIG. 5. The initial rates of P450 inactivation caused by the secondary amine (dark gray) or secondary hydroxylamine (light gray) in control experiments. The striped bars immediately to the right of each show the effect of coincubation with the primary amines of each series. The concentrations were as follows: DES-CYP2C11 series (50 μM DES, 1 μM DESOH, and 1 μM DDES); (*S*)-FLX-CYP2C19 series [10 μM (*S*)-FLX, 5 μM (*S*)-FLXOH, and 0.1 μM (*S*)-NFLX]; MA-CYP3A4 series (2 μM MA, 0.5 μM MAOH, and 0.2 μM MD). Primary amines caused significant ($p < 0.05$) inhibition of inactivation by the secondary amines and secondary hydroxylamines in all cases.

combined effects of tertiary amines and their secondary amine metabolites (Galetin et al., 2006; Zhang et al., 2009a,b). A key assumption implicit to these models is that the fates of the relevant downstream metabolites (hydroxylamines, nitrones, and nitroso compounds) formed in vivo are reproduced in the in vitro experiments, which are used to generate the apparent kinetic parameters (K_I and k_{inact}). A second assumption of these models is that the contribution of these metabolites in the promotion or inhibition of enzyme inactivation is known.

The metabolic scheme for the formation of MI complexes from tertiary alkyl amines includes multiple pathways and branching reactions that complicate analysis even in single enzyme systems (Fig. 1). Here, the metabolism of secondary amines to primary amines and secondary hydroxylamines was studied. There is ample literature precedent to show that metabolism of these two products of secondary amine metabolism can lead to the formation of MI complexes. The rates of MI complex formation by a secondary amine and its primary metabolites, where each step in the pathway is catalyzed by the same enzyme, have not been directly compared in single enzyme systems. We examined three secondary amine-enzyme systems: DES-CYP2C11, (*S*)-FLX-CYP2C19, and MA-CYP3A4. In each case, incubation of the secondary amines with their respective P450 enzyme caused rapid formation of MI complexes. The relative rates of MI complex formation followed the order secondary hydroxylamine > secondary amine $\gg$ primary amine (Fig. 3). Of particular note, MI complex formation by the primary amines was slow and incomplete. We also found that the primary amines inhibit rather than promote enzyme inactivation caused by the secondary amines. Lindeke et al. (1979) suggested that

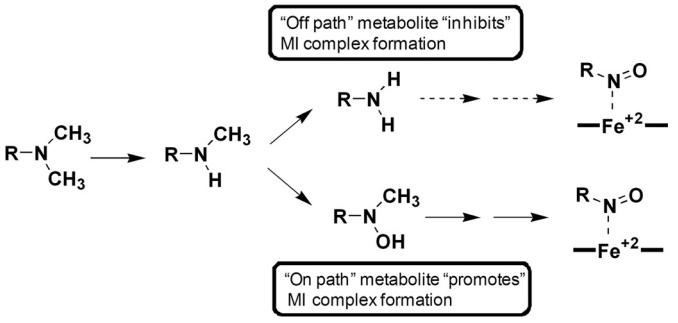

FIG. 6. The major roles of the primary amine and secondary hydroxylamine metabolites in the metabolism of the three secondary amines to MI complexes. The formation of MI complexes occurs via the secondary hydroxylamine pathway. Formation of MI complexes by the primary amine pathway is negligible. The primary amine metabolites accumulate in incubations to significant levels that cause significant inhibition of MI complex formation by the secondary amines.

the formation of MI complexes in rat liver microsomes by *N*-methylamphetamine arises via the secondary hydroxylamine pathway rather than via the formation of the primary amine. Likewise, Jeffery and Mannering (1983) concluded that MI complex formation from the metabolism of *N*-benzylamphetamine arises via the secondary hydroxylamine pathway rather than through the formation of the primary amine. By these criteria and the literature precedent, we propose that the secondary hydroxylamine metabolites, rather than the primary amines from DES, (*S*)-FLX, and MA, are on the major pathway to MI complex formation.

Two additional lines of evidence support this conclusion. First, the secondary hydroxylamines (DESOH, (*S*)-FLXOH, and MAOH) are observed as metabolites of the secondary amines. The formation of DESOH from imipramine and desipramine has been demonstrated in rabbit liver microsomes (Beckett et al., 1983), whereas (*S*)-FLXOH and MAOH are newly identified metabolites. Second, deuterium substitution on the methyl group of DES results in a 2-fold reduction of formation of DDES from DES by CYP2C11 but has no significant effect on the final concentration of DESOH or the MI complex. Furthermore, there is no significant isotope effect on the initial rate of MI complex formation, which rules out a significant contribution of the primary amine pathway to MI complex formation.

The factors that govern the rates of formation of the primary amine and secondary hydroxylamine metabolites from a secondary amine will be important determinants of the formation rates for MI complexes and the magnitude of DDIs caused by alkyl amines. The clearance of primary amines can be slow, and primary amine metabolites can accumulate in vivo. The *N*-hydroxylation reaction, on the other hand, has received less mechanistic attention and the fate of hydroxylamines in vivo and in vitro is not well understood. In addition, although *N*-dealkylation is generally catalyzed by P450 enzymes, *N*-hydroxylation reactions may be catalyzed by other enzymes present in more complex systems such as microsomes, hepatocytes, and the intact liver. For example, it has been shown that the formation of an MI complex in microsomes by a secondary cyclopropylamine required the flavin-containing monooxygenase-catalyzed conversion to a secondary hydroxylamine (Cerny and Hanzlik, 2005).

Little information about the product ratios and reaction rates for the generation of primary amines and secondary hydroxylamines from secondary amines by P450 enzymes has been reported. However, data are available that suggest that *N*-hydroxylation and *N*-dealkylation are mechanistically linked. For instance, metabolism of the *N*-ethylamphetamine isomers results in a ratio of *N*-dealkylation to *N*-hydroxy-

lation (sum of secondary hydroxylamine and ethylene nitrone) of 5:1 for the (*S*)-enantiomer and 3:1 for the (*R*)-enantiomer in rabbit liver microsomes (Beckett and Haya, 1978). In addition, the metabolism of methamphetamine by five purified rat enzymes results in product ratios (primary amine/secondary hydroxylamine) that range from 2 (CYP2B2) to 14 (CYP1A1) (Baba et al., 1988). The branching ratio estimates calculated from our studies [primary amine/(secondary hydroxylamine + MI complex)] range from less than 1 (MA-CYP3A4 = 0.8) to 3.6 [(*S*)-FLX-CYP2C19]. Multiple P450 enzymes, including CYP3A4, CYP2C9, and CYP2D6, catalyze the *N*-demethylation of the fluoxetine isomers. In addition, we have found that *N*-demethylation is always accompanied by *N*-hydroxylation in single enzyme systems and in microsomes (B. M. VandenBrink and K. L. Kunze, unpublished data). Theoretical calculations for the P450-catalyzed oxidation of trimethylamine and dimethylaniline to the corresponding secondary amines and *N*-oxides indicate that *N*-demethylation and *N*-oxygenation are both catalyzed by the perferryl oxygen. *N*-Dealkylation is predicted to be favored over *N*-oxygenation by 2.6 kcal/mol (Chunsen et al., 2009). The above experimental results for the analogous P450-catalyzed reactions with secondary amines indicate that the difference in activation energies for the two competing reactions is low and variable with enzyme and substrate.

MI complex formation by DES, (*S*)-FLX, and MA is inhibited by the corresponding primary amine metabolites. Significant inhibition of MI complex formation by the primary amine metabolites would be expected to influence the progress curves for MI complex formation. Silverman (1988) considered the possibility that a metabolite of a conventional one-step mechanism-based inhibitor will have a significant affinity for the enzyme and concluded that the observed rate of inactivation will be time-dependent. The resulting conventional semilog plots will, in some cases, be curved as reproduced in Fig. 7. Likewise, Zhang et al. (2009a) have considered the combined effects of tertiary amines and their secondary amine metabolites in vitro and in vivo and concluded that both species (e.g., diltiazem and MA) must be explicitly considered as substrates and inhibitors of inactivation to achieve accurate predictions. Our data show that the models may need to be modified to incorporate terms that account for the effects of the primary amine metabolites and that reflect the roles of the other branched metabolites.

Although our results favor MI complex formation through the secondary hydroxylamine metabolite, the fact that primary amines can cause formation of MI complexes is well established. One example for which the primary amine pathway may be more important is in the formation of MI complexes by *N*-desmethylclarithromycin and *N,N*-didesmethylclarithromycin in dexamethazone-induced rat liver microsomes. In this instance, the rates of MI complex formation seem to be similar for the primary and secondary amines incubated at the same concentration (Ohmori et al., 1993). The cycloalkylamine substructure of clarithromycin and erythromycin may selectively promote the primary hydroxylamine pathway. This possibility is supported by studies with analogs of the amphetamine series, which clearly demonstrate that the rate of MI complex formation by primary amines is increased by the presence of a branched lipophilic group on the α-carbon of the alkyl amine (Lindeke et al., 1982). Although structure-activity relationship studies have not been reported for the corresponding effects of α-carbon substitution on the conversion of secondary amines to MI complexes and/or secondary hydroxylamines, studies in microsomes also show that substitution on the α-carbon substantially increase catalytic efficiency (V_{max}/K_m) for *N*-demethylation of secondary amines (Duncan et al., 1983). Thus, it is feasible that the presence of branched lipophilic groups on the α-carbon, exemplified by the cycloalkylamine structures of erythromycin and clarithromycin, will serve to increase the likelihood that the primary amine pathway will contribute to MI complex formation.

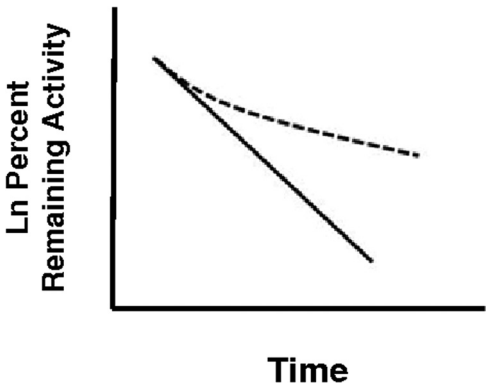

FIG. 7. Hypothetical semilog plots that show the effect of the accumulation of a branched "off path" metabolite on enzyme inactivation for a classic one-step mechanism-based inhibition (MBI). Significant metabolite accumulation causes the normal first-order plot (solid line) to be nonlinear (dashed line). [This figure has been drawn on the basis of a plot provided by Silverman (1988).]

Fluoxetine causes TDI of CYP2C19 activity in Supersomes, HLMs, hepatocytes, and profound inhibition in vivo (McGinnity et al., 2006). Thus, we conclude that the inactivation of CYP2C19 both in vitro and most likely in vivo is due to formation of the secondary hydroxylamine metabolite of fluoxetine, which subsequently forms an MI complex to inactivate the enzyme. The CYP3A4-diltiazem interaction has received considerable clinical, experimental, and theoretical attention. We conclude that formation of an MI complex with CYP3A4 in vitro and possibly in vivo is through the secondary hydroxylamine metabolite of diltiazem. In addition, we show that the primary amine metabolite protects CYP3A4 from MI complex formation by accumulating in solution and competing for active enzyme (K_i = 0.2 μM) (Zhao et al., 2007). However, similar roles in vivo cannot be assigned to these metabolites because the fate of the primary amine and secondary hydroxylamine of diltiazem is unknown.

These studies show that secondary hydroxylamine metabolites of DES, (*S*)-FLX, and MA promote P450 MI complex formation. In these cases, the primary amine metabolites inhibit MI complex formation. Further characterization of alkyl amine metabolism by P450 enzymes in single enzyme and multiple enzyme preparations is necessary before establishment of guidelines for prediction. It seems prudent to include studies in hepatocytes, in which the metabolites are exposed to the full complement of enzymes, when seeking to eliminate or confirm the possibility of DDIs with alkyl amines (Zhao et al., 2005; McGinnity et al., 2006). Levels of primary amines and hydroxylamines in vitro and in vivo may be significantly different, and the prediction of primary and secondary metabolite concentrations in vivo from in vitro data is problematic at best and warrants further investigation.

Acknowledgments. We acknowledge Tom Kalhorn for help in development of the LC-MS and LC-MS/MS assays. We thank Ping Zhao for helpful discussions regarding this work.

References

Alexander J (1993) A convenient preparation of N-demethyldiltiazem and its conversion to a diltiazem homolog. *Org Prep Proced Int* **25:**133–137.

Baba T, Yamada H, Oguri K, and Yoshimura H (1988) Participation of cytochrome P-450 isozymes in N-demethylation, N-hydroxylation and aromatic hydroxylation of methamphetamine. *Xenobiotica* **18:**475–484.

Backman JT, Olkkola KT, Aranko K, Himberg JJ, and Neuvonen PJ (1994) Dose of midazolam should be reduced during diltiazem and verapamil treatments. *Br J Clin Pharmacol* **37:**221–225.

Beckett AH and Haya K (1978) The stereoselective metabolism of ethylamphetamine with fortified rabbit liver homogenates. *Xenobiotica* **8:**85–96.

Beckett AH, Hutt AJ, and Navas GE (1983) Metabolism of imipramine in vitro: synthesis and characterization of N-hydroxydesmethylimipramine. *Xenobiotica* **13:**391–405.
Bensoussan C, Delaforge M, and Mansuy D (1995) Particular ability of cytochrome P450 3A to form inhibitory P450-iron-metabolite complexes upon metabolic oxidation of aminodrugs. *Biochem Pharmacol* **49:**591–602.
Buening MK and Franklin MR (1976) The formation of cytochrome P-450-metabolic intermediate complexes in microsomal fractions from extrahepatic tissues of the rabbit. *Drug Metab Dispos* **4:**556–561.
Cerny MA and Hanzlik RP (2005) Cyclopropylamine inactivation of cytochromes P450: role of metabolic intermediate complexes. *Arch Biochem Biophys* **436:**265–275.
Chunsen L, Wei W, Kyung-Bin C, and Sason S (2009) Oxidation of tertiary amines by cytochrome P450—kinetic isotope effect as a spin-state reactivity probe. *Chem Eur J* **15:**8492–8503.
Corey EJ and Reichard GA (1989) Enantioselective and practical syntheses of *R*- and *S*-fluoxetines. *Tetrahedron Lett* **30:**5207–5210.
Correia MA and Ortiz de Montellano PR (2005) *Cytochrome P450: Structure, Mechanism, and Biochemistry*, 3rd ed (Ortiz de Montellano PR ed) pp 263–267, Kluwer Academic/Plenum Publishers, New York.
Di Marco A, Cellucci A, Chaudhary A, Fonsi M, and Laufer R (2007) High-throughput radiometric CYP2C19 inhibition assay using tritiated (*S*)-mephenytoin. *Drug Metab Dispos* **35:**1737–1743.
Duncan JD, Hallström G, Paulsen-Sörman U, Lindeke B, and Cho AK (1983) Effects of α-carbon substituents on the *N*-demethylation of *N*-methyl-2-phenethylamines by rat liver microsomes. *Drug Metab Dispos* **11:**15–20.
Franklin MR (1974) The formation of a 455 nm complex during cytochrome P-450-dependent *N*-hydroxyamphetamine metabolism. *Mol Pharm* **10:**975–985.
Franklin MR (1995) Enhanced rates of cytochrome P450 metabolic-intermediate complex formation from nonmacrolide amines in rifampicin-treated rabbit liver microsomes. *Drug Metab Dispos* **23:**1379–1382.
Galetin A, Burt H, Gibbons L, and Houston JB (2006) Prediction of time-dependent CYP3A4 drug-drug interactions: impact of enzyme degradation, parallel elimination pathways, and intestinal inhibition. *Drug Metab Dispos* **34:**166–175.
Gumbrecht JR and Franklin MR (1979) The formation of cytochrome P-450-metabolic intermediate complexes from amines, in the isolated perfused rat liver. *Xenobiotica* **9:**547–554.
Hall J, Naranjo CA, Sproule BA, and Herrmann N (2003) Pharmacokinetic and pharmacodynamic evaluation of the inhibition of alprazolam by citalopram and fluoxetine. *J Clin Psychopharmacol* **23:**349–357.
Hilborn JW, Lu Z-H, Jurgens AR, Fang QK, Byers P, Wald SA, and Senanayake CH (2001) A practical asymmetric synthesis of (*R*)-fluoxetine and its major metabolite (*R*)-norfluoxetine. *Tetrahedon Lett* **42:**8919–8921.
Jeffery EH and Mannering GJ (1983) Interaction of constitutive and phenobarbital-induced cytochrome P-450 isozymes during the sequential oxidation of benzphetamine. Explanation for the difference in benzphetamine-induced hydrogen peroxide production and 455-nm complex formation in microsomes from untreated and phenobarbital-treated rats. *Mol Pharmacol* **23:**748–757.
Jönsson KH and Lindeke B (1992) Cytochrome P-455 nm complex formation in the metabolism of phenylalkylamines. XII. Enantioselectivity and temperature dependence in microsomes and reconstituted cytochrome P-450 systems from rat liver. *Chirality* **4:**469–477.
Kamal A, Khanna GBR, and Ramu R (2002) Chemoenzymatic synthesis of both enantiomers of fluoxetine, tomoxetine and nisoxetine: lipase-catalyzed resolution of 3-aryl-3-hydroxypropanenitriles. *Tetrahedron Asymm* **13:**2039–2051.
Kawalek JC, Levin W, Ryan D, and Lu AY (1976) Reconstituted liver microsomal enzyme system that hydroxylates drugs, other foreign compounds, and endogenous substrates. IX. The formation of a 455-nm metabolite-cytochrome P-450 complex. *Drug Metab Dispos* **4:**190–194.
Kurebayashi H (1989) Kinetic deuterium isotope effects on deamination and N-hydroxylation of cyclohexylamine by rabbit liver microsomes. *Arch Biochem Biophys* **270:**320–329.
Lindeke B, Paulsen U, and Anderson E (1979) Cytochrome P-455 complex formation in the metabolism of phenylalkylamines–IV. Spectral evidences for metabolic conversion of methamphetamine to N-hydroxyamphetamine. *Biochem Pharmacol* **28:**3629–3635.
Lindeke B, Paulsen-Sörman U, Hallström G, Khuthier AH, Cho AK, and Kammerer RC (1982) Cytochrome P-455-nm complex formation in the metabolism of phenylalkylamines. VI. Structure-activity relationships in metabolic intermediary complex formation with a series of α-substituted 2-phenylethylamines and corresponding *N*-hydroxylamines. *Drug Metab Dispos* **10:**700–705.
Liu Z and Franklin MR (1985) Cytochrome P-450 ligands: metyrapone revisited. *Arch Biochem Biophys* **241:**397–402.
Mayhew BS, Jones DR, and Hall SD (2000) An in vitro model for predicting in vivo inhibition of cytochrome P450 3A4 by metabolic intermediate complex formation. *Drug Metab Dispos* **28:**1031–1037.
McGinnity DF, Berry AJ, Kenny JR, Grime K, and Riley RJ (2006) Evaluation of time-dependent cytochrome P450 inhibition using cultured human hepatocytes. *Drug Metab Dispos* **34:**1291–1300.
Mitchell D and Koening TM (1995) Synthesis of R- and S- fluoxetine, norfluoxetine and related compounds from styrene oxide. *Syn Commun* **25:**1231–1238.
O'Neil IA, Cleator E, and Tapolczay DJ (2001) A convenient synthesis of secondary hydroxylamines. *Tetrahedron Lett* **42:**8247–8249.
Ohmori S, Ishii I, Kuriya S, Taniguchi T, Rikihisa T, Hirose S, Kanakubo Y, and Kitada M (1993) Effects of clarithromycin and its metabolites on the mixed function oxidase system in hepatic microsomes of rats. *Drug Metab Dispos* **21:**358–363.
Polasek TM and Miners JO (2008) Time-dependent inhibition of human drug metabolizing cytochromes P450 by tricyclic antidepressants. *Br J Clin Pharmacol* **65:**87–97.
Silverman RB (1988) *Mechanism-Based Enzyme Inactivation: Chemistry and Enzymology*, pp 1–30, CRC Press, Boca Raton, FL.
Zhang X, Galinsky RE, Kimura RE, Quinney SK, Jones DR, and Hall SD (2010) Inhibition of CYP3A by erythromycin: in vitro-in vivo correlation in rats. *Drug Metab Dispos* **38:**61–72.
Zhang X, Jones DR, and Hall SD (2009a) Prediction of the effect of erythromycin, diltiazem, and their metabolites, alone and in combination, on CYP3A4 inhibition. *Drug Metab Dispos* **37:**150–160.
Zhang X, Quinney SK, Gorski JC, Jones DR, and Hall SD (2009b) Semiphysiologically based pharmacokinetic models for the inhibition of midazolam clearance by diltiazem and its major metabolite. *Drug Metab Dispos* **37:**1587–1597.
Zhao P, Kunze KL, and Lee CA (2005) Evaluation of time-dependent inactivation of CYP3A in cryopreserved human hepatocytes. *Drug Metab Dispos* **33:**853–861.
Zhao P, Lee CA, and Kunze KL (2007) Sequential metabolism is responsible for diltiazem-induced time-dependent loss of CYP3A. *Drug Metab Dispos* **35:**704–712.

Address correspondence to: Dr. Kent L. Kunze, Department of Medicinal Chemistry, University of Washington, Box 357610, Seattle, WA 98195. E-mail: kkunze@u.washington.edu